REGULAR ARTICLE

blood advances

# LSD1 defines erythroleukemia metabolism by controlling the lineage-specific transcription factors GATA1 and C/EBPα

Kensaku Kohrogi,[1,2] Shinjiro Hino,[1] Akihisa Sakamoto,[1] Kotaro Anan,[1,2] Ryuta Takase,[1] Hirotaka Araki,[1] Yuko Hino,[1] Kazutaka Araki,[3] Tetsuya Sato,[4] Kimitoshi Nakamura,[2] and Mitsuyoshi Nakao[1]

[1]Department of Medical Cell Biology, Institute of Molecular Embryology and Genetics, and [2]Department of Pediatrics, Graduate School of Medical Sciences, Kumamoto University, Kumamoto, Japan; [3]Biological Data Science Research Group, Cellular and Molecular Biotechnology Research Institute, National Institute of Advanced Industrial Science and Technology, Tokyo, Japan; and [4]Division of Bioinformatics, Medical Institute of Bioregulation, Kyushu University, Fukuoka, Japan

Downloaded from http://ashpublications.net/bloodadvances/article-pdf/5/9/2305/1806172/advancesadv2020003521.pdf by guest on 08 June 2024

**Key Points**

- EL cells show activated glycolysis and high expression of LSD1 among the AML subtypes, which represent unique metabolic phenotypes.
- LSD1 promotes glycolysis and heme synthesis by stabilizing GATA1 and maintains GATA1-target metabolic genes by downregulating C/EBPα.

Acute myeloid leukemia (AML) is a heterogenous malignancy characterized by distinct lineage subtypes and various genetic/epigenetic alterations. As with other neoplasms, AML cells have well-known aerobic glycolysis, but metabolic variations depending on cellular lineages also exist. Lysine-specific demethylase-1 (LSD1) has been reported to be crucial for human leukemogenesis, which is currently one of the emerging therapeutic targets. However, metabolic roles of LSD1 and lineage-dependent factors remain to be elucidated in AML cells. Here, we show that LSD1 directs a hematopoietic lineage-specific metabolic program in AML subtypes. Erythroid leukemia (EL) cells particularly showed activated glycolysis and high expression of LSD1 in both AML cell lines and clinical samples. Transcriptome, chromatin immunoprecipitation–sequencing, and metabolomic analyses revealed that LSD1 was essential not only for glycolysis but also for heme synthesis, the most characteristic metabolic pathway of erythroid origin. Notably, LSD1 stabilized the erythroid transcription factor GATA1, which directly enhanced the expression of glycolysis and heme synthesis genes. In contrast, LSD1 epigenetically downregulated the granulo-monocytic transcription factor C/EBPα. Thus, the use of LSD1 knockdown or chemical inhibitor dominated C/EBPα instead of GATA1 in EL cells, resulting in metabolic shifts and growth arrest. Furthermore, GATA1 suppressed the gene encoding C/EBPα that then acted as a repressor of GATA1 target genes. Collectively, we conclude that LSD1 shapes metabolic phenotypes in EL cells by balancing these lineage-specific transcription factors and that LSD1 inhibitors pharmacologically cause lineage-dependent metabolic remodeling.

## Introduction

Although aerobic glycolysis has been thought of as a common hallmark of cancer,[1] emerging evidence suggests the existence of metabolic heterogeneity within and between tumor types, and this could be a potential barrier in targeting metabolic vulnerability in cancer therapies.[2-7] Acute myeloid leukemia (AML) is a group of hematopoietic malignancies comprising many subtypes with different lineage identities and genetic/epigenetic lesions.[8,9] Although the characteristic differences among subtypes have been described, variable metabolic phenotypes and their regulatory mechanisms remain unexplored. A previous report, using an MLL-AF9 AML model in mice, showed that leukemic cells are more vulnerable to perturbations of glycolytic genes than normal hematopoietic cells.[10] Another

Submitted 1 October 2020; accepted 17 March 2021; published online 30 April 2021. DOI 10.1182/bloodadvances.2020003521.

The data reported in this article have been deposited in the Gene Expression Omnibus database (accession numbers GSM145397 [RNA-seq], GSE145399 [histones], and GSE145401 [LSD1]).

Requests by other investigators regarding materials, data sets, and protocols may be submitted to the corresponding authors (Shinjiro Hino [s-hino@kumamoto-u.ac.jp] or Mitsuyoshi Nakao [mnakao@gpo.kumamoto-u.ac.jp]).

The full-text version of this article contains a data supplement.

© 2021 by The American Society of Hematology

report has shown a similar glycolysis dependency in AML cells harboring internal tandem repeats of the *FLT3* gene.[11] In addition, mutations in the isocitrate dehydrogenase gene generate a rare metabolite that causes epigenetic disruption in AML.[12] Because these observations are limited to subtypes with specific genotypes, it remains unclear whether lineage differences are linked to metabolic properties in AML. In addition, the availability of nutrients such as glucose and glutamine exerts a profound influence on the cell fate decision during normal hematopoiesis.[13] These observations raise the possibility that metabolic phenotypes and/or nutrient requirements vary among AML subtypes depending on lineage identities. Despite remarkable clinical advances, there is considerable variability in the success of therapy among AML subtypes.[8,14] Thus, targeting of subtype-specific metabolic features could provide a powerful tool for next-generation AML therapy.

Lysine-specific demethylase-1 (LSD1) was first identified as a histone H3 lysine 4 (H3K4) demethylase and later as a demethylase for transcription factors (TFs) such as p53 and STAT3.[15,16] LSD1 has been implicated in diverse biological processes, including cellular differentiation, tumor development, and metabolism.[17,18] We previously reported that, in hepatocellular carcinoma cells, LSD1 represses mitochondrial respiration-associated genes such as *PPARGC1A* through H3K4 demethylation, while promoting the expression of glycolytic genes by facilitating hypoxia-inducible factor-1α (HIF-1α)–mediated transcription.[19] In addition, high expression of LSD1 is associated with enhanced glucose uptake in human esophageal cancer.[20] In hematopoietic cells, LSD1 physically interacts and cooperates with growth factor independence-1 and growth factor independence-1b, TFs that are involved in multiple steps of hematopoiesis.[21] The depletion of LSD1 in the hematopoietic system results in defects in stem and progenitor cells, thereby impeding the differentiation of multiple lineages.[22] Increased expression of LSD1 has been observed in many different types of human hematopoietic neoplasms, implying significant involvement in leukemogenesis.[23] Indeed, small compound inhibitors of LSD1 have been shown to eradicate leukemic cells effectively.[24-27]

In this study, we investigated the role of LSD1 in metabolic regulation in human AML subtypes and found that erythroid leukemia (EL) cells have activated glycolysis and high expression of LSD1. Using transcriptomic and epigenomic approaches, we identified that LSD1 facilitates the function of the erythroid-specific factor GATA1, while suppressing the granulo-monocytic factor C/EBPα. In addition, we found that GATA1 and C/EBPα work in a mutually exclusive manner in EL cells, emphasizing a functional balance of these lineage-dependent TFs by LSD1. We therefore concluded that LSD1 plays essential roles in the metabolic heterogeneity of AML and especially in metabolic phenotypes of EL cells.

# Methods

## Cell culture

AML cell lines (HEL, TF1a, SET-2, NB4, and HL60) and K562 cells were grown in RPMI 1640 medium (Sigma), supplemented with 10% heat-inactivated fetal bovine serum, 50 U/mL penicillin, and 50 μg/mL streptomycin at 37°C with 95% air and 5% carbon dioxide. Detailed information on cell lines is provided in supplemental Table 1. Hemoglobin synthesis in HEL cells was induced by the addition of 30 μM hemin for 4 days and visualized by benzidine staining as described previously.[28]

## Lentiviral expression of short hairpin RNA

Lentiviral vectors for tetracycline-inducible short hairpin RNA expression were obtained from the RIKEN BioResource Research Center (http://cfm.brc.riken.jp/Lentiviral_Vectors_J). The short hairpin RNA target sequences were as follows: shLSD1_#1, 5′-CACAAGGAAAGCTAGAAGA-3′; shLSD1_#2, 5′-AACAATTAGAAGCACCTTA-3′; shGATA1, 5′-GGATGGTATTCAGACTCGA-3′; shCEBPA, 5′-ACGAGACGTCCATCGACAT-3′; shALAS2_#1, 5′-GATGTGAAGGCTTTCAAGA-3′; shALAS2_#2, 5′-AGGCTTCATCTTTACCACT-3′; shGATA2, 5′-GAAGTGTCTCCTGACCCTA-3′; and shGFI1 5′-GCTCGGAGTTTGAGGACTTCT-3′.

## Measurement of cellular glucose uptake

To measure glucose uptake, cells were incubated in the culture medium containing 100 μM 2-NBDG (Peptide Institute) for 2 hours, as previously described.[29]

## Real-time measurement of glycolytic activity

Monitoring of cellular glycolytic activity was performed by using the XFe24 Extracellular Flux analyzer (Seahorse Bioscience). For floating cells, we used Cellbed (Japan Vilene), a high-purity silica fiber that can be used as a three-dimensional cell culture scaffold sheet on each well of the assay plate (300 000 cells per well). To evaluate glycolysis capacity, cells were cultured in glucose-free medium for 1 hour before the assay. Real-time measurement was initiated under glucose-free conditions, followed by the addition of 25 mM glucose and then a glycolysis inhibitor 2-deoxy-glucose at 100 mM. Glycolytic flux was determined by measuring the extracellular acidification rate.

## Metabolomic analyses

Metabolomic analyses were conducted by using capillary electrophoresis time of flight mass spectrometry at Human Metabolome Technologies. Cluster analyses were performed as previously described.[30] The amount of metabolite was normalized for hierarchical clustering by the average linking method using Cluster 3.0. The heatmap was visualized by Java Tree view. In supplemental Figure 4L, 57 metabolites were detected in our experiment and registered in the Cancer Cell Encyclopedia (CCLE) database.[7]

## Poly (A) RNA-sequencing analysis

Total RNA from HEL cells was extracted by using the RNeasy Mini Kit (Qiagen). Messenger RNA (mRNA) was purified by using an NEBNext Poly (A) mRNA Magnetic Isolation Module (NEB). A complementary DNA library was synthesized by using a NEBNext Ultra DNA Library Prep Kit for Illumina (NEB) and was sequenced on a NextSeq 500 sequencer (Illumina) with 75 bp single-end reads. The resulting reads were aligned to the UCSC hg19 reference genome by using TopHat (version 1.4.1).[31] Normalization, differential analysis, gene ontology analysis, and construction of the Venn diagram were performed by using Strand NGS (Strand Genomics). The primers used for quantitative reverse transcription polymerase chain reaction (RT-qPCR) to confirm gene expression are listed in supplemental Table 2.

Downloaded from http://ashpublications.net/bloodadvances/article-pdf/5/9/2305/1806172/advancesadv2020003521.pdf by guest on 08 June 2024

### Chromatin immunoprecipitation

About $8 \times 10^6$ and $4 \times 10^6$ HEL cells were used to detect methylated histone H3K4 and LSD1 enrichment, and GATA1 enrichment, respectively. Crosslinking, fragmentation, and chromatin immunoprecipitation (ChIP) experiments were performed with some modifications (supplemental Methods) based on previous reports.[32,33] The primers used are listed in supplemental Table 2.

### ChIP-sequencing analysis

Using $8 \times 10^6$ HEL cells, ChIP experiments were performed as noted earlier, and each protein-bound chromatin fraction was collected for DNA purification. Library preparation was done by using the NEBNext Ultra II DNA Library Kit for Illumina (New England Biolabs). Adapter-ligated DNA fragments were purified by using Agencourt AMPure XP. High-throughput sequencing was performed by using a NextSeq 500 Sequencer with 75 bp single-end reads. The qualified reads were aligned onto the human reference genome hg19 by using the Burrows-Wheeler Alignment algorithm.[34] Duplicate reads and the reads with low overall quality or low mapping quality were excluded. The final numbers of mapped reads are listed in supplemental Table 3. Peak detection was done by using the MACS2 algorithm. For LSD1/ChIP-sequencing, sequencing data from duplicate samples were separately mapped to the genome, merged, and then subjected to peak calling with MACS2 algorithm. Motif analyses and peak annotations were done with HOMER.[35] Peaks within intergenic regions were associated with nearby genes if they were within a 100-kb window from the transcriptional start site of a specific gene. The cooccupancy of LSD1 with other proteins was analyzed by using ChIP-Atlas (http://chip-atlas.org/). Visualization of ChIP-sequencing data was done by using the Integrative Genomics Viewer (http://software.broadinstitute.org/software/igv/) after converting BAM files into bigWig files. ChIP-sequencing for H3K9me3 in K562 cells was obtained from the ENCODE/Broad Institute via the UCSC Genome Browser Web site (http://genome.ucsc.edu/index.html).

### Clinical data sets

Transcriptome data set from clinical AML cases were obtained from The Cancer Genome Atlas (TCGA) database (https://www.cancer.gov/about-nci/organization/ccg/research/structural-genomics/tcga). Transcriptome data from EL (AML-M6) cases were obtained from the St. Jude PeCan Data Portal88 (https://pecan.stjude.cloud/proteinpaint/study/ael).[36] These data sets use different algorithms for the normalization of expression levels (TCGA, transcripts per million; St. Jude PeCan Data Portal88, counts per million). Therefore, to analyze these data sets collectively, we normalized the expression level of each gene to an internal control. A gene encoding TATA-binding protein (*TBP*) was selected for this purpose because it showed relatively low sample-to-sample variation compared with other candidates such as *RPLP0* and *ACTB*.

### Statistical analysis and reproducibility

Data are presented as the mean ± standard deviation. Equality of variance was examined by using an F test. All statistical analyses were performed by using a two-tailed Student's *t* test. A value of $P < .05$ was considered statistically significant. Representative data/images were replicated in at least 3 independent experiments.

## Results

### High expression of LSD1 is directly linked to enhanced glucose metabolism in EL

To examine whether LSD1 contributes to enhanced glycolysis in leukemic cells, we analyzed the gene expression profiles of AML cell lines and clinical samples using publicly available data sets from the TCGA and the CCLE.[37,38] Expression of *LSD1* and *GLUT1* (*SLC2A1*), a major regulator of glucose flux, was significantly and positively correlated in both cell lines and clinical samples (Figure 1A-B; supplemental Figure 1A). In particular, these genes were highly expressed in EL, which is classified as a unique subtype of AML (FAB M6).[39,40] An analysis of a published single-cell RNA-sequencing data[41] from normal hematopoietic cells revealed enhanced expression of LSD1 in the erythroid lineage (e-ery and l-ery) (supplemental Figure 1B). Notably, LSD1-high EL cells with different genetic backgrounds exhibited higher levels of medium acidification and GLUT1 expression than did other AML cells (Figure 1C; supplemental Figure 1C-D; supplemental Table 1), indicating that enhanced glycolysis is a characteristic of erythroid lineage. To test the function of LSD1 in metabolic regulation, we generated doxycycline-inducible LSD1-knockdown (KD) cells using distinct EL cell lines, HEL and TF1a. LSD1-KD downregulated the expression of *GLUT1* as well as *PKLR*, an essential glycolytic enzyme in erythroid cells (Figure 1D-E; supplemental Figure 1E-H).[42] Consistent with the gene expression profiles, LSD1-KD cells showed reduced glucose uptake and glycolytic capacity (Figure 1F-G; supplemental Figure 1I-K).

Treatment with S2101, a selective inhibitor of LSD1, led to similar gene expression and metabolic changes (Figure 1H-K; supplemental Figure 2A-D). These results were reproduced by the use of alternative LSD1 inhibitors, T-3775440 and GSK-LSD1 (supplemental Figure 2E-J). Moreover, LSD1 inhibition selectively inhibited the growth of EL and megakaryoblastic leukemia cells, which exhibited high LSD1 expression (Figure 1B; supplemental 3). In non-EL AML cells, *GLUT1* expression was mostly unaffected by LSD1 inhibition (supplemental Figure 2K). The data show that increased LSD1 in the EL subtype is directly linked to enhanced glycolytic activities.

### LSD1 facilitates metabolic pathways associated with erythroid lineage

To further identify LSD1-dependent metabolic pathways in EL cells, we analyzed the gene expression changes in LSD1-inhibited HEL cells by RNA-sequencing. We identified that 334 genes were commonly downregulated by both LSD1-KD and S2101 treatment (Figure 2A). Of note, genes involved in heme biosynthesis were commonly downregulated by LSD1 inhibition. By qRT-PCR, we confirmed that key genes in heme metabolism such as *ALAS2* and *SLC25A37* (encoding 5′-aminolevulinate synthase-2 and mitoferrin-1, respectively) were significantly downregulated in LSD1-inhibited HEL and TF1a cells (Figure 2C; supplemental Figure 4A-F). To test the essentiality of heme synthesis in EL cells, we generated ALAS2-KD HEL cells. ALAS2-KD resulted in reduced cell growth, when combined with $Fe^{2+}$ depletion by deferoxamine, an iron chelator, suggesting that the heme synthetic pathway is involved in survival and/or growth (supplemental Figure 4G-I). Because heme synthesis is intimately associated with erythrocyte function, we hypothesized that LSD1 directs a lineage-linked metabolic phenotype. To test this

Downloaded from http://ashpublications.net/bloodadvances/article-pdf/5/9/2305/1806172/advancesadv2020003521.pdf by guest on 08 June 2024

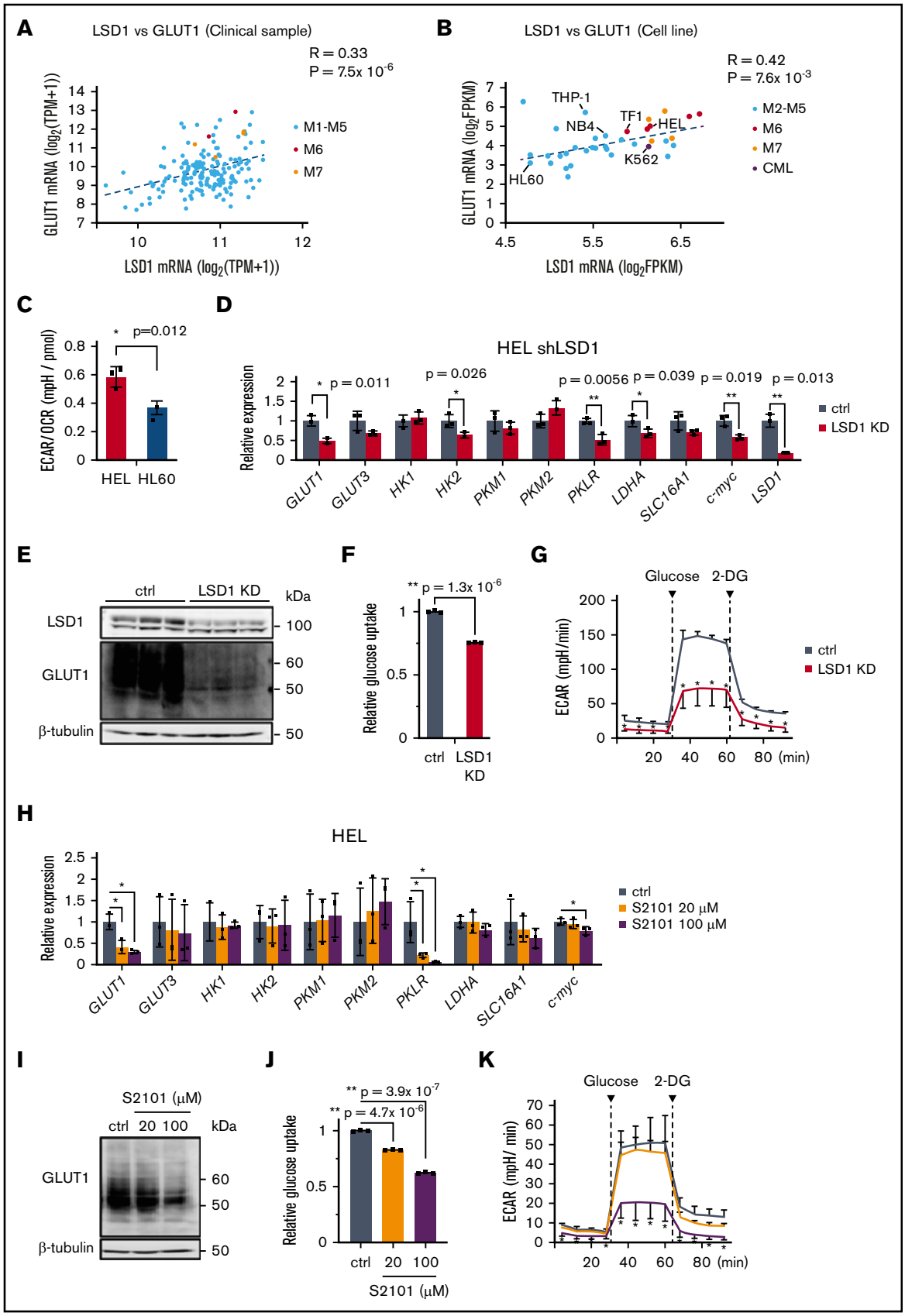


Figure 1.

Downloaded from http://ashpublications.net/bloodadvances/article-pdf/5/9/2305/1806172/advancesadv2020003521.pdf by guest on 08 June 2024

theory, we analyzed metabolic properties in LSD1-inhibited cells after treatment with hemin, a chemical that promotes erythroid characteristics. Consistent with the gene expression changes, hemin-induced hemoglobin production was downregulated by the loss of LSD1 (Figure 2D; supplemental Figure 4J). It is important to note that LSD1-inhibited cells did not exhibit morphologic changes (supplemental Figure 4K), suggesting that differentiation status was not altered. Enhancement of erythroid-type metabolism by hemin was confirmed by a metabolomic examination, in which hemin treatment led to increases in the EL-enriched metabolites (supplemental Figure 4L), based on the CCLE metabolome database.[7] We found that such hemin-induced increases of metabolites were mostly canceled by treatment with S2101 (Figure 2E). Collectively, these data suggest that LSD1 directs an erythroid-associated metabolic phenotype in EL cells.

In our RNA-sequencing data, 409 genes were upregulated by LSD1-KD and S2101 treatment (Figure 2B). Many of these genes were associated with membrane-bound proteins. Among these genes, *CD48* and *CD34*, which are surface markers of lymphocytes and hematopoietic stem cells, respectively, were prominently upregulated by LSD1 inhibition (Figures 2F-G, 4A). These data indicate that LSD1 suppresses non-erythroid features in EL cells.

## LSD1 cooperates with GATA1 to promote metabolic gene expression

To gain mechanistic insight into metabolic gene regulation by LSD1, we examined the distribution of LSD1-bound sites in HEL cells by ChIP-sequencing analysis. Among the 8280 LSD1 ChIP peaks, 81% were located in introns and intergenic regions (Figure 3A). Motif analysis of LSD1-bound sites identified enrichment of consensus motifs for transcription factors such as the GATA family and RUNX family proteins (Figure 3B). The co-existence of LSD1- and GATA-bound sites was confirmed by comparing our ChIP-sequencing data with publicly available data sets using ChIP-Atlas (http://chip-atlas.org/) (supplemental Figure 5A).[43] The GATA family consists of GATA1-6, each having a unique expression pattern and function. In particular, deregulation of GATA1 function has been linked to impaired erythroid differentiation, and thus to leukemogenesis.[44] Interestingly, GATA1 was abundantly expressed in HEL cells (supplemental Figure 5B) and physically interacted with LSD1 (Figure 3C; supplemental Figure 5C), implying an active role of GATA1 in EL cells. To explore the role of GATA1 in metabolic regulation, we knocked down *GATA1* in HEL and TF1a cells and found remarkably reduced expression of *GLUT1* as well as a known GATA1-regulated gene, *ALAS2* (Figure 3D-E; supplemental Figure 5D-E). Consistently, GATA1-KD led to a downregulation of glucose uptake and extracellular acidification rate (Figure 3F-G). By ChIP-qPCR analyses, we found that GATA1 occupies putative enhancers of *GLUT1* and *ALAS2* genes (Figure 3H; supplemental Figure 5G-H). We also observed a growth reduction in GATA1-KD cells (Figure 3I; supplemental Figure 5F), indicating an essential role of GATA1 in cell maintenance. These data collectively suggest that GATA1 promotes glycolysis by directly regulating *GLUT1* expression in EL cells.

Notably, we found that the enrichment of GATA1 at *GLUT1* and *ALAS2* enhancers was abolished by LSD1 depletion (Figure 3H; supplemental Figure 5G-H). In addition, GATA1 protein decreased under LSD1 inhibition, while *GATA1* mRNA remained unaffected (Figure 3J; supplemental Figure 4E-F; supplemental Figure 5I-M), suggesting a posttranscriptional control of GATA1 by LSD1. Indeed, when a proteasome inhibitor (MG132) was used in combination with LSD1 inhibition, the reduction of GATA1 was canceled (Figure 3K; supplemental Figure 5K-M). Taken together, these data show that LSD1 protects GATA1 from proteasomal degradation, which in turn enhances glycolysis and heme synthesis in EL cells.

## LSD1 and GATA1 repress the myeloid-specific enhancer of *CEBPA*

Because LSD1 inhibition led to a derepression of non-erythroid hematopoietic genes (Figure 2B,F,G), we next investigated whether the suppression of nonerythroid features is important for metabolic phenotypes. Among the genes upregulated by LSD1 inhibition, the *CEBPA* gene, which encodes a key granulo-monocytic transcription factor C/EBPα, showed a dramatic increase (Figure 4A; supplemental Figure 6A-D). We confirmed that C/EBPα increased to levels comparable to those of myeloblastic leukemia cells (Figure 4B). Consistently, *CD11b*, a well-known myeloid marker, was markedly upregulated by LSD1 inhibition, indicative of a compromised erythroid identity (Figure 4C-D; supplemental Figure 6A-B). To gain mechanistic insights, by ChIP-sequencing analysis, we examined the effects of LSD1 inhibition on mono- and di-methylated H3K4 (H3K4me1 and me2) that are hallmarks of enhancer function (supplemental Figure 6E-G). Combination analyses of the ChIP-sequencing data revealed that LSD1-enriched sites were located close to the H3K4me1 and H3K4me2 peaks but not to the H3K9me3 peaks (data from K562

Downloaded from http://ashpublications.net/bloodadvances/article-pdf/5/9/2305/1806172/advancesadv2020003521.pdf by guest on 08 June 2024

**Figure 1. High levels of LSD1 expression and glycolytic activity in erythroleukemia cells.** Scatter plots showing positive correlation between *LSD1* and *GLUT1* expression in AML in TCGA clinical samples (n = 173) (A) and CCLE cell lines (n = 37) (B). Pearson product correlation coefficient and *P* values are indicated. (C) Glycolysis/OXPHOS balance of HEL and HL60 cells, determined by using an extracellular flux analyzer. Values indicate the ratio of extracellular acidification rate (ECAR) and oxygen consumption rate (OCR). Values are mean ± standard deviation (SD) of 10 wells. (D) Expression changes of glycolytic genes in HEL cells expressing short hairpin RNA against LSD1 (shLSD1#1). Full descriptions of gene symbols are provided in supplemental Table 2. qRT-PCR values, which were normalized to the expression levels of the 36B4 gene, are shown as the fold difference against control (ctrl) samples. (E) Decrease of GLUT1 protein was confirmed in LSD1-KD HEL cells. Scanned images of unprocessed blots are shown in supplemental Figure 10. (F) Reduction of glucose uptake in LSD1-KD HEL cells. 2-NBDG incorporation was determined by flow cytometry. Mean fluorescence intensities are shown. (G) Reduced glycolytic activity in LSD1-KD HEL cells. Values are mean ± SD of 5 assays. (H) Expression changes of glycolytic genes under the treatment with the LSD1 inhibitor S2101. (I) Decrease of GLUT1 protein in S2101-treated HEL cells. (J) Reduction of glucose uptake by S2101 treatment. (K) Reduction of glycolytic activity in S2101-treated HEL cells. Values are mean ± SD of 5 assays. All samples were collected at day 4 unless indicated otherwise. All histogram data are mean ± SD of triplicate results unless indicated otherwise. *$P < .05$, **$P < .01$ vs control. CMP, common myeloid progenitor; FPKM, fragments per kilobase of transcript per million mapped reads; GMP, granulocyte erythroid progenitor; HSC, hematopoietic stem cell; MEP, megakaryocyte erythroid progenitor.

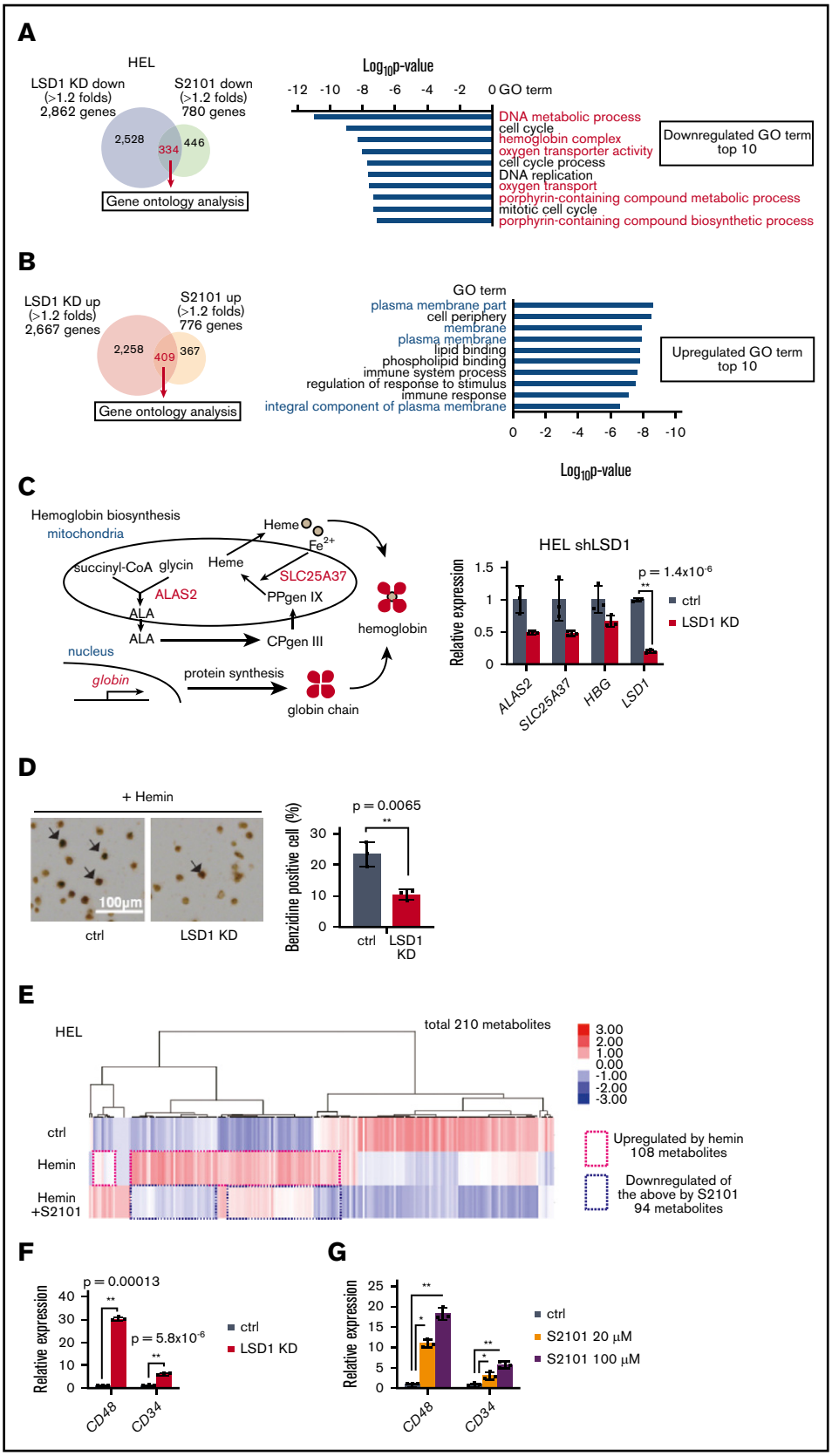


**Figure 2. LSD1 facilitates erythroid lineage-linked metabolic phenotype.** RNA-sequencing analysis. Venn diagrams of genes upregulated (A) and downregulated (B) more than 1.2-fold by LSD1-KD and S2101 treatment (10 μM) are indicated (left). Gene ontology (GO) analysis of the gene sets significantly upregulated and downregulated by LSD1 inhibition (right). Top 10 pathways with statistical significance are indicated with $\log_{10} P$ values. Pathways related to heme synthesis (upregulated) and membrane-bound proteins (downregulated) are highlighted in red and blue, respectively. (C) Schema of hemoglobin synthesis pathway (left). qRT-PCR data showing expression changes of hemoglobin biosynthesis genes in LSD1-KD HEL cells (right). (D) Light microscopy image of benzidine-stained HEL cells (left). Arrows represent benzidine-positive cells. Proportions of benzidine-positive cells (right). The experiment was triplicated by calculating 1000 cells in each assay. (E) Metabolomic analysis of LSD1-inhibited HEL cells. Cells were treated with hemin and S2101 and were subjected to capillary electrophoresis time of flight mass spectrometry–based metabolomic analysis. (F-G) Expression changes of non-erythroid hematopoietic markers in LSD1-KD– and S2101-treated HEL cells. All histogram data are mean ± standard deviation of triplicate results. *$P < .05$, **$P < .01$ vs control. ALA, 5′-aminolevulinic acid; CPgen III, coproporphyrinogen III; PP IX, protoporphyrin IX.

Downloaded from http://ashpublications.net/bloodadvances/article-pdf/5/9/2305/1806172/advancesadv2020003521.pdf by guest on 08 June 2024

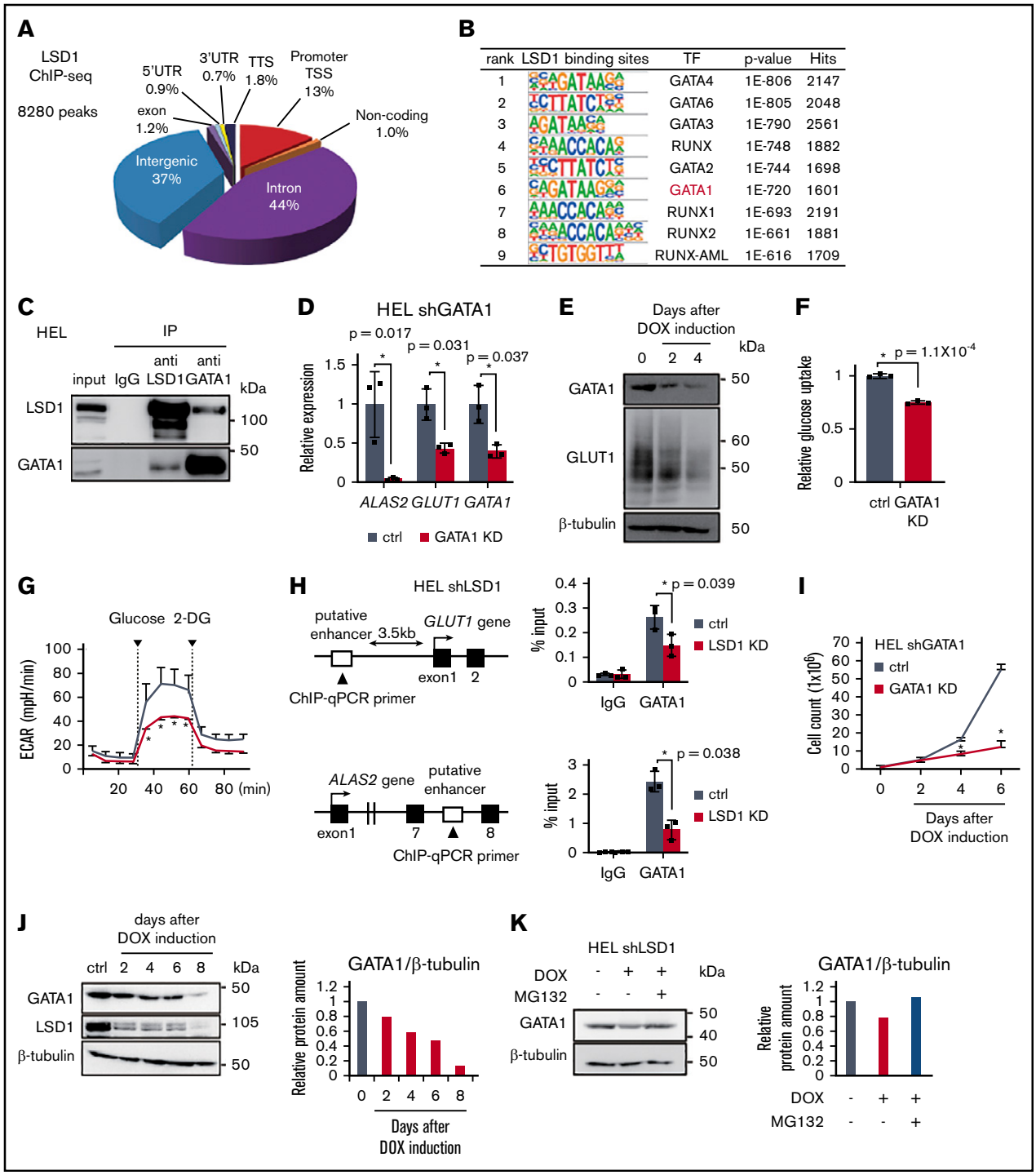


**Figure 3. LSD1 cooperates with GATA1 to promote glycolysis.** (A) ChIP-sequencing (ChIP-seq) analysis. Distribution of LSD1-enriched peaks in HEL cells, relative to annotated regions in the genome. (B) Motif analysis of 8280 LSD1-enriched peaks. Motif and statistical analyses were performed by using HOMER software. (C) Coimmunoprecipitation of LSD1 and GATA1. Input lane contains the 10% of the total amount of whole cell extract, relative to IP lanes. (D) Gene expression changes in GATA1-KD HEL cells. (E) Decreased GLUT1 protein in GATA1-KD HEL cells. Samples were collected at indicated days after doxycycline (DOX) induction. (F) Reduction of glucose uptake in GATA1-KD HEL cells, as determined by 2-NBDG incorporation. (G) Reduction of glycolytic activity in GATA1-KD HEL cells. Values are mean ± standard deviation of 5 assays. (H) LSD1-dependent enrichment of GATA1 at *ALAS2* and *GLUT1* gene enhancers. ChIP-qPCR analyses were performed in control (ctrl) and LSD1-KD HEL cells. Enrichment values were calculated as percentage of input DNA. (I) Growth curve of ctrl and GATA1-KD HEL cells. (J) Downregulation of GATA1 protein in LSD1-KD HEL cells. Samples were collected at indicated days after DOX induction. (K) Effect of proteasome inhibition on GATA1 protein in LSD1-KD cells. The cells were treated with MG132 (10 μM) for 6 hours before harvest. Values are mean ± standard deviation of triplicate results except for those in panel G. $*P < .05$, $**P < .01$. 5′UTR, 5′ untranslated region; IgG, immunoglobulin G; TSS, transcriptional start site; TTS: transcriptional termination site.

Downloaded from http://ashpublications.net/bloodadvances/article-pdf/5/9/2305/1806172/advancesadv2020003521.pdf by guest on 08 June 2024

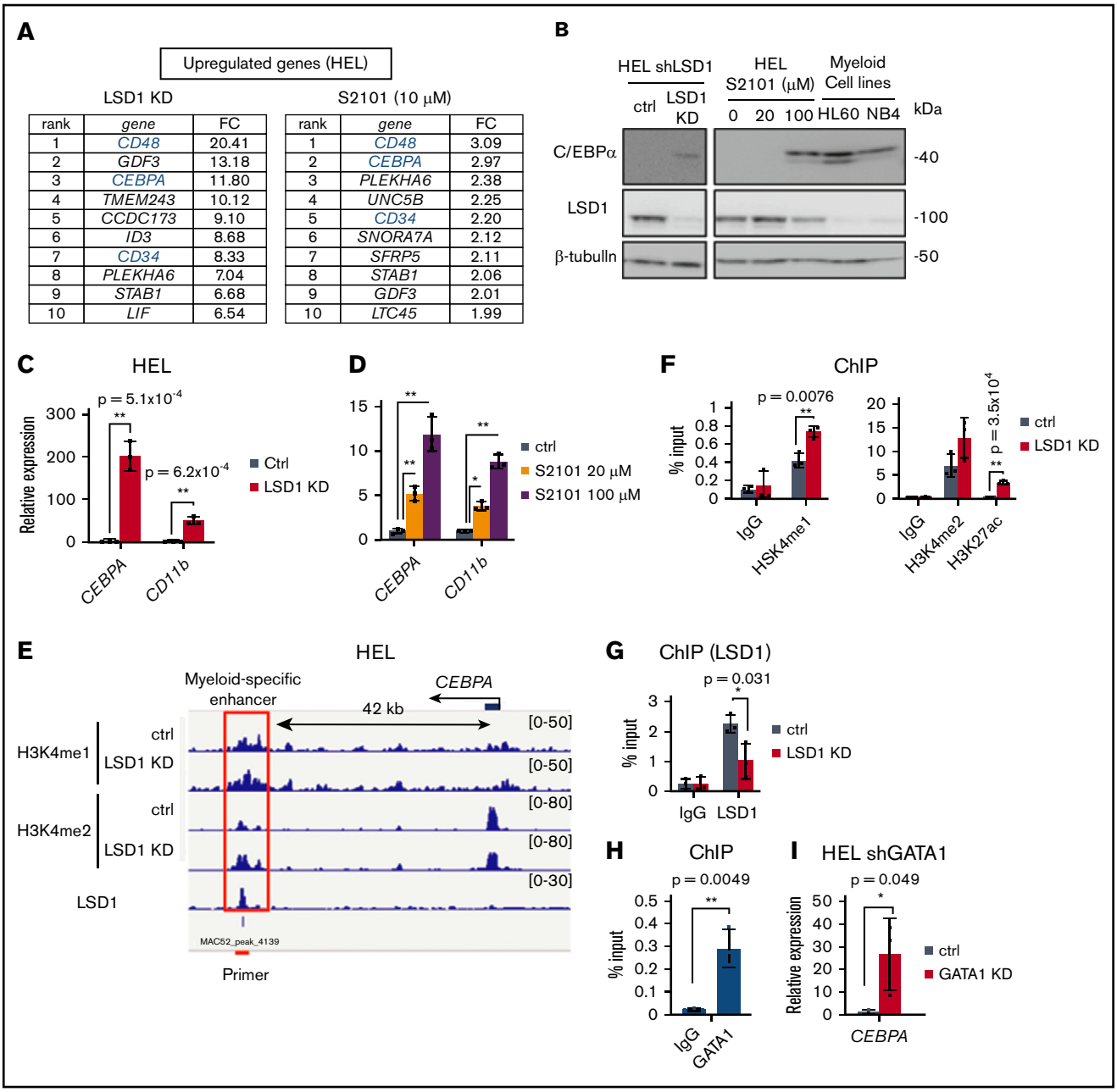


**Figure 4. LSD1 represses a myeloid-specific enhancer of the *CEBPA* gene via H3K4 demethylation.** (A) Top 10 upregulated genes by LSD1 inhibition. Fold change (FC) values relative to untreated control are indicated. (B) Expression of C/EBPα protein in LSD1-KD– and S2101-treated HEL cells. (C-D) Expression changes of myeloid-related genes in LSD1-KD– and S2101-treated HEL cells. (E) Enrichment of H3K4me1, H3K4me2, and LSD1 at the *CEBPA* gene locus by ChIP-sequencing analysis. LSD1-KD data are also indicated. Red line indicates the ChIP-qPCR primer at the myeloid-specific enhancer. Data were visualized by using Integrative Genomics Viewer (http://software.broadinstitute.org/software/igv/). (F) Increase of H3K4me1, H3K4me2, and H3K27ac at the *CEBPA* enhancer by LSD1-KD. ChIP-qPCR signals were calculated relative to that of histone H3. (G) Enrichment of LSD1 at *CEBPA* enhancer examined by ChIP-qPCR. (H) Enrichment of GATA1 at the*CEBPA* enhancer in HEL cells tested by ChIP-qPCR. Enrichment values at the enhancer were normalized to input DNAs for panels F to H. (I) Upregulation of *CEBPA* in GATA1-KD HEL cells. Values are mean ± standard deviation of triplicate results. $^{*}P < .05$, $^{**}P < .01$.

cells) (supplemental Figure 6E-F). Consistent with the H3K4 demethylating activity, LSD1-KD elevated the levels of H3K4me1 and H3K4me2 near the LSD1-enriched sites (supplemental Figure 6G). An LSD1-KD–induced increase of H3K4me1 and me2 was found at 42 kb downstream of the *CEBPA* transcription start site, a region that has been reported as a myeloid-specific enhancer of this gene (Figure 4E).[45] By ChIP-qPCR, we confirmed the increase of methylated H3K4 as well as H3K27ac, a mark of active enhancers, by LSD1-KD (Figure 4F; supplemental Figure 6H-J). Importantly, we found an occupancy of LSD1 in this region (Figure 4E-G), suggesting that LSD1 directly represses the *CEBPA* enhancer through H3K4 demethylation. Notably, GATA1 was also



Downloaded from http://ashpublications.net/bloodadvances/article-pdf/5/9/2305/1806172/advancesadv2020003521.pdf by guest on 08 June 2024

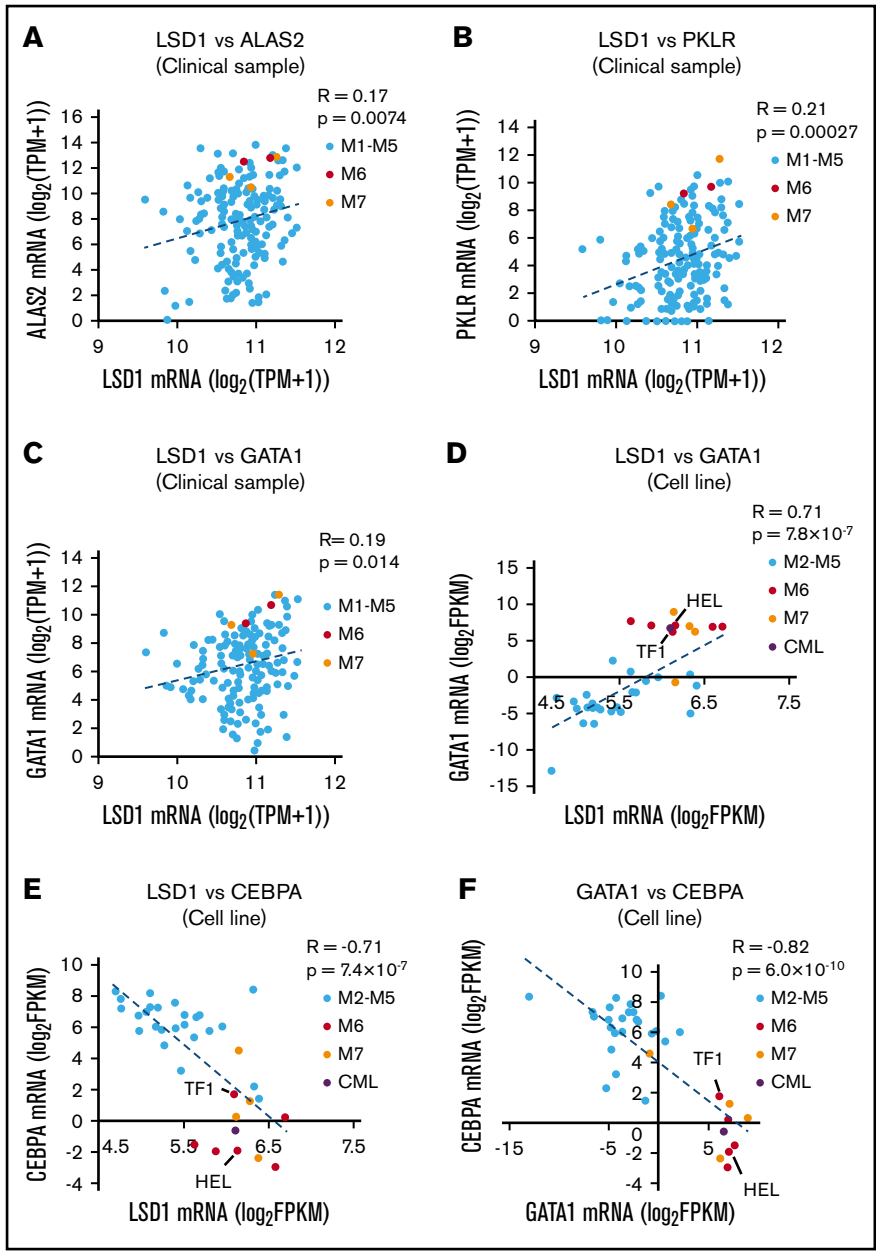


**Figure 5. LSD1 expression is correlated positively with metabolic and *GATA1* genes and negatively with *CEBPA* gene in AML cells of erythroid and megakaryocytic lineages.** Scatter plots showing positive correlation of *LSD1* and *ALAS2* (A), *LSD1* and *PKLR* (B), and *LSD1* and *GATA1* (C) in AML clinical samples in the TCGA database (n = 173). (D) Scatter plots showing positive correlation between *LSD1* and *GATA1* in AML cell lines (CCLE, n = 37). Scatter plots showing inverse correlation between *LSD1* and *CEBPA* (E) and between *GATA1* and *CEBPA* (F) in AML cell lines (CCLE, n = 37). Pearson product correlation coefficient and *P* values are indicated.

present in this region (Figure 4H; supplemental Figure 6K), and its KD led to a remarkable upregulation of *CEBPA* expression (Figure 4I). The data collectively revealed that LSD1 and GATA1 together repress the *CEBPA* gene, contributing to the maintenance of erythroid cell identity.

## LSD1 expression is correlated positively with metabolic and *GATA1* genes and negatively with the*CEBPA* gene in EL cells

We found that LSD1 promotes glycolysis and heme synthesis by facilitating GATA1 function in EL cells (Figure 3). To gain a broader view of the LSD1-dependent metabolic program in AML, we analyzed publicly available transcriptome data sets. In clinical AML samples (data from TCGA), *LSD1* and its downstream metabolic genes such as *ALAS2* and *PKLR* were coexpressed with significant correlation, and M6/M7 leukemic cells particularly showed high expression of both genes (Figure 5A-B; red and yellow dots). In addition, *LSD1* and *GATA1* genes were highly coexpressed in M6/M7 cells among AML subtypes (Figure 5C-D), suggesting the cooperative control of LSD1 and GATA1 in EL cells at both protein and mRNA levels. Furthermore, consistent with our experimental data in Figure 4, the expression of *CEBPA* was negatively correlated with those of *LSD1* and *GATA1*, particularly in M6/M7 cells among AML cell lines (data from CCLE) (Figure 5E-F).

To further evaluate the relevance of LSD1 in metabolic traits in EL, we made use of a published data set that consists of transcriptome profiles of 141 AML-M6 cases.[36] Expression of *GLUT1* and *LSD1* was mildly correlated, whereas *LSD1* expression did not correlate

Downloaded from http://ashpublications.net/bloodadvances/article-pdf/5/9/2305/1806172/advancesadv2020003521.pdf by guest on 08 June 2024

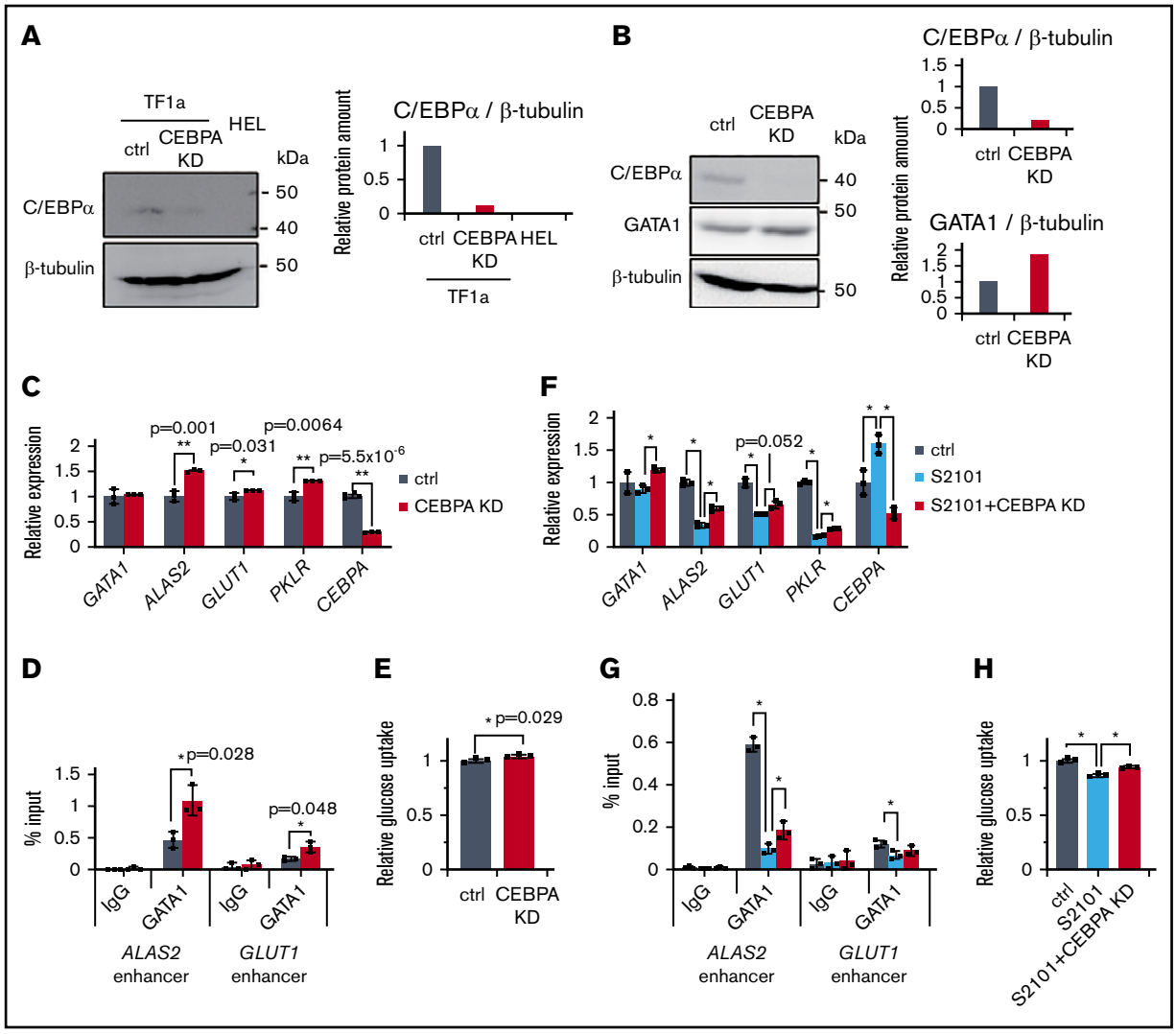


**Figure 6. C/EBPα interferes with GATA1-dependent metabolic program.** (A) Expression of C/EBPα protein in TF1a and HEL. It is noteworthy that C/EBPα was detectable in TF1a but not in HEL cells under basal conditions (left). Intensities of C/EBPα bands were quantified by densitometry and normalized to those for β-tubulin (right). (B) Increased GATA1 in CEBPA-KD TF1a cells. CEBPA-KD upregulated GATA1 protein. (C) Expression changes of LSD1 target genes in CEBPA-KD TF1a cells. (D) Increased enrichment of GATA1 at the *ALAS2* and *GLUT1* enhancers in CEBPA-KD TF1a cells. (E) Increased glucose uptake in CEBPA-KD TF1a cells. (F) Expression changes of LSD1 target genes in S2101 treated and CEBPA-KD TF1a cells. Concentration of S2101 is 50 μM. (G) GATA1 enrichments at *ALAS2* and *GLUT1* enhancers in S2101-treated and CEBPA-KD TF1a cells. Enrichment values at the enhancers were normalized to input DNA for panels D and G. (H) Restored glucose uptake by CEBPA-KD in S2101-treated TF1a cells. S2101 was used at 20 μM. Values are mean ± standard deviation of triplicate results. **P* < .05, ***P* < .01.

with *ALAS2* within the M6 cases studied (supplemental Figure 7A-B). We found significant positive correlations of *LSD1* with *PKLR* and *GATA1*, consistent with our in vitro observations (supplemental Figure 7C-D). In addition, *CEBPA* was negatively correlated with both *LSD1* and *GATA1* (supplemental Figure 7E-F). We then sought to compare these M6 cases with the non-M6 cases in the TCGA data set (n = 171). Consistent with their lineage identities, the 2 groups showed distinct expression of *GATA1*, *CEBPA*, and *PU.1* (normalized to an internal control, *TBP*) (supplemental Figure 7G). Scatter plot analyses revealed that enhanced expression of *LSD1* coexisted with high expression of *GLUT1*, *ALAS2*, and *GATA1* in the M6 group (supplemental Figure 7H-J), whereas *CEBPA* expression was low in the same group (supplemental Figure 7K).

We next explored the possible role of LSD1 in metabolic variation at the single-cell level using a published single-cell RNA-sequencing data set from patients with AML; malignant cells in this data set were classified by hallmark AML mutations.[41] Of interest, we found that when leukemic cells were divided into subpopulations according to genotypes (mutations in *FLT3*, *NPM1*, *DNMT3*, and *p53* genes), there were no obvious differences in the metabolic gene expression (supplemental Figure 8A). Using the same data set, we found that the expression of LSD1 was correlated with those of lineage and metabolic genes in both normal and malignant cell populations (supplemental Figure 8B-C). These data further emphasize the essential roles of LSD1 in shaping lineage-dependent metabolic phenotypes in AML cells.

Downloaded from http://ashpublications.net/bloodadvances/article-pdf/5/9/2305/1806172/advancesadv2020003521.pdf by guest on 08 June 2024

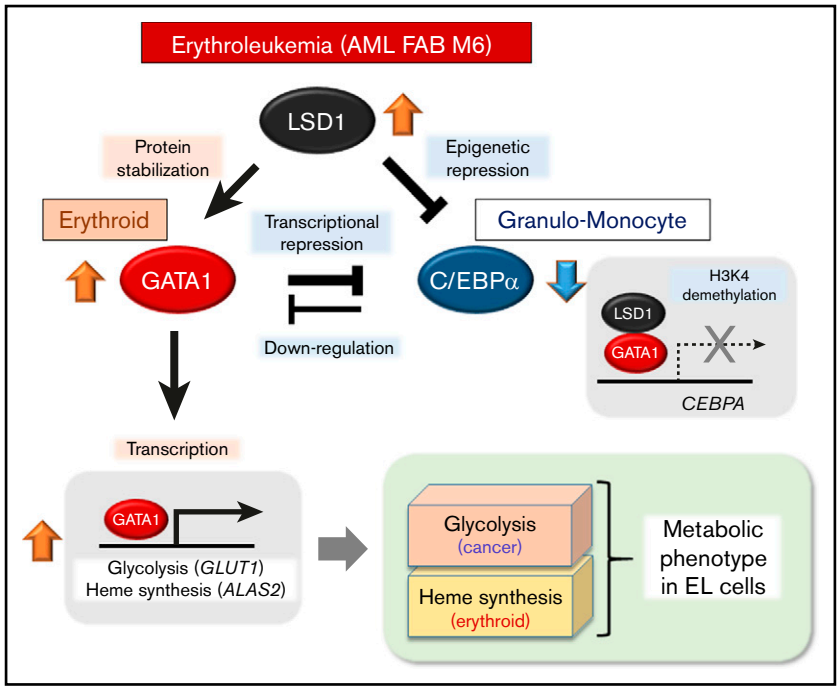


**Figure 7. Schematic model: control of lineage TF balance by LSD1 defines the metabolic phenotype in EL cells.** Overexpressed LSD1 stabilizes GATA1, which activates glycolysis and heme biosynthesis genes while LSD1 suppresses *CEBPA* expression via H3K4 demethylation. Lineage-specific transcription factors GATA1 and C/EBPα are mutually restraining. Therefore, LSD1 inhibition derepresses *CEBPA* expression and down-regulates GATA1 function, leading to metabolic remodeling and growth arrest.

### C/EBPα interferes with GATA1-dependent metabolic pathways

Although C/EBPα is known to primarily contribute to myeloid differentiation, the role of this protein in leukemic metabolism has not been investigated. To test this, we knocked down *CEBPA* in TF1a cells that expressed a detectable basal amount of the endogenous C/EBPα among EL cell lines (Figure 6A). Interestingly, the loss of C/EBPα increased GATA1 protein about twice (Figure 6B). GATA1-targeted metabolic genes such as *ALAS2* and *GLUT1* were upregulated by CEBPA-KD, with enhanced enrichment of GATA1 at its target enhancers (Figure 6C-D). Consistent with the gene expression changes, glucose uptake was small but significantly augmented by CEBPA-KD (Figure 6E).

We next investigated whether C/EBPα participates in metabolic reprogramming under LSD1 inhibition, using a combination of S2101 and CEBPA-KD. In this setting, we confirmed that the induction of *CEBPA* expression by S2101 was completely abolished by CEBPA-KD (Figure 6F). Importantly, CEBPA-KD reversed downregulation of metabolic genes, including *GLUT1* under LSD1 inhibition, with a partial recovery of GATA1 binding at target enhancers (Figure 6F-G). Consistent with this finding, glucose uptake in LSD1-inhibited cells was restored by CEBPA-KD (Figure 6H). The results suggest that C/EBPα suppresses GATA1 function and thereby remodels the metabolic phenotype in EL cells.

Finally, we tested the involvement of other transcriptional regulators that are associated with erythroid lineage and LSD1 function. GATA2 is known to operate at an early phase of erythroid maturation before GATA1 expression.[46] In our GATA2-KD experiments in HEL cells, there were no changes in glucose uptake, glycolytic activity, or the expression of heme synthesis genes (supplemental Figure 9A-D), suggesting that these metabolic pathways are specifically regulated by GATA1. We then performed KD of GFI1, a transcriptional repressor known to cooperate with LSD1.[47] Although some of the metabolic genes were affected by GFI1-KD, glucose uptake and glycolytic activity remained unchanged (supplemental Figure 9E-H). In our preliminary proteomic study in HEL cells, we did not find bindings of LSD1 with TAL1, JARID1A, LDB1, or LMO2, which are known to cooperate with LSD1 and/or GATA1 (data not shown).[48,49] Taken together, these data suggest a unique mode of metabolic gene regulation by the LSD1/GATA1 axis.

## Discussion

In the current study, we showed that LSD1 regulates both GATA1 and C/EBPα, which directly control lineage-specific and key metabolic genes in EL cells among AML subtypes. Specifically, LSD1 facilitates the function of an erythroid TF, GATA1, while repressing a granulo-monocytic TF, C/EBPα (Figure 7). As a consequence, dominance of GATA1 over C/EBPα drives the expression of EL-dependent metabolic genes such as those involved in glycolysis and heme synthesis. Because expression of LSD1 was highly correlated with that of metabolic genes across AML subtypes, balancing of lineage TFs by LSD1 likely has a broad impact on the metabolic diversification in AML. A recent report showed that biallelic *CEBPA* mutation combined with heterozygous mutation in *GATA2* induce EL in mice.[50] In these mutant mice, myeloid progenitors, which ectopically expressed erythroid TFs including GATA1, underwent malignant transformation. Thus, during EL development, disrupted balance of lineage TFs (possibly induced by LSD1) may trigger metabolic reprogramming.

Enhanced glucose utilization is a hallmark of many tumor cells. In fact, myc and HIF-1α, TFs that are commonly activated in tumors, have been implicated in glycolytic activation.[51] We and others have previously shown that LSD1 promotes glycolysis by increasing the stability of HIF-1α.[19,52] In EL cells, we found no involvement of LSD1 in stabilizing HIF-1α (data not shown). Instead, we showed

Downloaded from http://ashpublications.net/bloodadvances/article-pdf/5/9/2305/1806172/advancesadv2020003521.pdf by guest on 08 June 2024

that LSD1 cooperates with GATA1 to transcriptionally activate key glucose metabolism genes. These observations suggest that LSD1 is widely involved in aerobic glycolysis by using distinct sets of TFs in various cancer types.

We found that GATA1 directly controls EL-associated metabolism and is essential for cell growth. Our findings may be seemingly contradictory to a previous report showing that attenuated expression of GATA1 induces erythroid leukemia.[53] However, the authors in the same paper described that residual expression of GATA1 contributed to malignancy. In recent reports, either a gain of GATA1-interfering factor or a loss of GATA1-collaborator impeded normal erythropoiesis and generated EL-like states in mice,[54,55] suggesting that, while losing erythropoietic capacity, GATA1 acquires an alternative function during EL development. Thus, a reasonable explanation of our findings is that LSD1 potentiates the leukemogenic function of GATA1 to generate a unique metabolic phenotype in EL. Mechanistically, we found that LSD1 binds to and stabilizes GATA1 at the protein level. Previous reports showed that GATA1 is susceptible to caspase-mediated proteolysis and is protected by HSP70,[56] and that HSP27 protects GATA1 from proteasomal degradation.[57] Because we showed that proteasome inhibition restored GATA1 under LSD1 inhibition, LSD1 may modulate GATA1 status via the function of THE HSP pathway. Because we observed increased GATA1 protein by CEBPA-KD (Figure 6B), C/EBPα might also be involved in these pathways via transcriptional regulation.

C/EBPα is essential for the differentiation of granulocytes and monocytes.[58] In a subset of AML expressing RUNX1-fusion oncoproteins, forced expression of C/EBPα is sufficient to reverse aberrant epigenetic programs associated with the undifferentiated leukemic state.[59] In leukemic B-cell lines, forced expression of C/EBPα induced trans-differentiation into the macrophage lineage and reduced the tumorigenicity.[60] Furthermore, inactivating mutations in the *CEBPA* gene have been detected at a high frequency in AML,[61] suggesting that C/EBPα acts as a tumor suppressor in hematopoietic cells. Here, we found that the induction of C/EBPα in LSD1-inhibited cells led to the downregulation of glycolysis and heme synthesis genes. Thus, C/EBPα deficiency may induce metabolic reprogramming associated with differentiation blockade and malignant phenotypes in AML.

It is important to note that EL cells with different genetic mutations exhibited enhanced glycolytic activities. Notably, our transcriptome and metabolome data from different AML subtypes indicated that glycolytic activity was highly dependent on LSD1 and GATA1 but not on the gene mutation types. This evidence indicates that lineage identity has a significant impact on shaping the metabolic phenotypes in AML. Nonetheless, accumulating data suggests that genetic background is a major determinant of AML characteristics, and that specific mutations have been implicated in metabolic features.[62,63] Thus, lineage identity and genetic lesions may cooperatively direct metabolic reprogramming that allows AML cells to develop optimal survival strategies.

Clinical trials for the treatment of AML with LSD1 inhibitors have been implemented with promising outcomes.[64] EL cases with enhanced LSD1 expression may be highly sensitive to this treatment. In this study, we showed that disruption of heme synthesis by ALAS2-KD enhanced the toxicity of an iron chelator, deferoxamine (supplemental Figure 4G). Because *ALAS2* expression is regulated by LSD1/GATA1 axis, LSD1 inhibition combined with disruption of iron metabolism may effectively attack metabolic vulnerability in EL. Targeting lineage-specific metabolic features combined with LSD1 inhibition may contribute to a highly selective eradication of AML cells.

## Acknowledgments

This work was supported by the following funding sources: JSPS KAKENHI (grants JP18H02618 and 18K19479 [M.N.]; 20H04108, JP16K07215, and 25430178 [S.H.]; and 20K16335 [K.K.]), Takeda Science Foundation (M.N. and S.H.), The SGH Foundation (S.H.), and the Japan Agency for Medical Research and Development (JP16gm0510007) (M.N.).

## Authorship

Contribution: K.K., S.H., and M.N. designed research; K.K., S.H., A.S., K. Anan, R.T., H.A., K. Araki, and Y.H. performed research; K.K., S.H., and T.S. analyzed data; K.K., S.H., and M.N. wrote the paper; and K.N. and M.N. supervised the study.

Conflict-of-interest disclosure: The authors declare no competing financial interests.

ORCID profiles: K.K., 0000-0001-6691-5439; K. Anan, 0000-0001-8370-6292; R.T., 0000-0003-2860-2647; Kazutaka Araki, 0000-0003-2901-2454; K.N., 0000-0003-4903-2428; M.N., 0000-0002-2196-8673.

Correspondence: Shinjiro Hino, Department of Medical Cell Biology, Institute of Molecular Embryology and Genetics, Kumamoto University 2-2-1 Honjo, Chuo-ku, Kumamoto 860-0811, Japan; e-mail: s-hino@kumamoto-u.ac.jp; or Mitsuyoshi Nakao, Department of Medical Cell Biology, Institute of Molecular Embryology and Genetics, Kumamoto University 2-2-1 Honjo, Chuo-ku, Kumamoto 860-0811, Japan; e-mail: mnakao@gpo.kumamoto-u.ac.jp.

## References

1. Pavlova NN, Thompson CB. The emerging hallmarks of cancer metabolism. *Cell Metab*. 2016;23(1):27-47.
2. Strickaert A, Saiselet M, Dom G, et al. Cancer heterogeneity is not compatible with one unique cancer cell metabolic map. *Oncogene*. 2017;36(19):2637-2642.
3. Chen PH, Cai L, Huffman K, et al. Metabolic diversity in human non-small cell lung cancer cells. *Mol Cell*. 2019;76(5):838-851.e5.
4. Intlekofer AM, Finley LWS. Metabolic signatures of cancer cells and stem cells. *Nat Metab*. 2019;1(2):177-188.
5. Garraway LA, Sellers WR. Lineage dependency and lineage-survival oncogenes in human cancer [published correction appears in *Nat Rev Cancer*. 2006;6(9):742]. *Nat Rev Cancer*. 2006;6(8):593-602.

Downloaded from http://ashpublications.net/bloodadvances/article-pdf/5/9/2305/1806172/advancesadv2020003521.pdf by guest on 08 June 2024

6. Yuneva MO, Fan TWM, Allen TD, et al. The metabolic profile of tumors depends on both the responsible genetic lesion and tissue type. *Cell Metab*. 2012; 15(2):157-170.
7. Li H, Ning S, Ghandi M, et al. The landscape of cancer cell line metabolism. *Nat Med*. 2019;25(5):850-860.
8. Döhner H, Estey EH, Amadori S, et al; European LeukemiaNet. Diagnosis and management of acute myeloid leukemia in adults: recommendations from an international expert panel, on behalf of the European LeukemiaNet. *Blood*. 2010;115(3):453-474.
9. Krause DS, Van Etten RA. Right on target: eradicating leukemic stem cells. *Trends Mol Med*. 2007;13(11):470-481.
10. Wang YH, Israelsen WJ, Lee D, et al. Cell-state-specific metabolic dependency in hematopoiesis and leukemogenesis. *Cell*. 2014;158(6):1309-1323.
11. Ju HQ, Zhan G, Huang A, et al. ITD mutation in FLT3 tyrosine kinase promotes Warburg effect and renders therapeutic sensitivity to glycolytic inhibition. *Leukemia*. 2017;31(10):2143-2150.
12. Xu W, Yang H, Liu Y, et al. Oncometabolite 2-hydroxyglutarate is a competitive inhibitor of α-ketoglutarate-dependent dioxygenases. *Cancer Cell*. 2011; 19(1):17-30.
13. Oburoglu L, Tardito S, Fritz V, et al. Glucose and glutamine metabolism regulate human hematopoietic stem cell lineage specification [published correction appears in *Cell Stem Cell*. 2014;15(5):666-8]. *Cell Stem Cell*. 2014;15(2):169-184.
14. Hossain MJ, Xie L, Caywood EH. Prognostic factors of childhood and adolescent acute myeloid leukemia (AML) survival: evidence from four decades of US population data. *Cancer Epidemiol*. 2015;39(5):720-726.
15. Huang J, Sengupta R, Espejo AB, et al. p53 Is regulated by the lysine demethylase LSD1. *Nature*. 2007;449(7158):105-108.
16. Yang J, Huang J, Dasgupta M, et al. Reversible methylation of promoter-bound STAT3 by histone-modifying enzymes. *Proc Natl Acad Sci USA*. 2010; 107(50):21499-21504.
17. Hino S, Kohrogi K, Nakao M. Histone demethylase LSD1 controls the phenotypic plasticity of cancer cells. *Cancer Sci*. 2016;107(9):1187-1192.
18. Nakao M, Anan K, Araki H, Hino S. Distinct roles of the $NAD^+$-Sirt1 and FAD-LSD1 pathways in metabolic response and tissue development. *Trends Endocrinol Metab*. 2019;30(7):409-412.
19. Sakamoto A, Hino S, Nagaoka K, et al. Lysine demethylase LSD1 coordinates glycolytic and mitochondrial metabolism in hepatocellular carcinoma cells. *Cancer Res*. 2015;75(7):1445-1456.
20. Kosumi K, Baba Y, Sakamoto A, et al. Lysine-specific demethylase-1 contributes to malignant behavior by regulation of invasive activity and metabolic shift in esophageal cancer. *Int J Cancer*. 2016;138(2):428-439.
21. Saleque S, Kim J, Rooke HM, Orkin SH. Epigenetic regulation of hematopoietic differentiation by Gfi-1 and Gfi-1b is mediated by the cofactors CoREST and LSD1. *Mol Cell*. 2007;27(4):562-572.
22. Kerenyi MA, Shao Z, Hsu YJ, et al. Histone demethylase Lsd1 represses hematopoietic stem and progenitor cell signatures during blood cell maturation. *eLife*. 2013;2:e00633.
23. Niebel D, Kirfel J, Janzen V, Höller T, Majores M, Gütgemann I. Lysine-specific demethylase 1 (LSD1) in hematopoietic and lymphoid neoplasms. *Blood*. 2014;124(1):151-152.
24. Schenk T, Chen WC, Göllner S, et al. Inhibition of the LSD1 (KDM1A) demethylase reactivates the all-trans-retinoic acid differentiation pathway in acute myeloid leukemia. *Nat Med*. 2012;18(4):605-611.
25. McGrath JP, Williamson KE, Balasubramanian S, et al. Pharmacological inhibition of the histone lysine demethylase KDM1A suppresses the growth of multiple acute myeloid leukemia subtypes. *Cancer Res*. 2016;76(7):1975-1988.
26. Ishikawa Y, Gamo K, Yabuki M, et al. A novel LSD1 inhibitor T-3775440 disrupts GFI1B-containing complex leading to transdifferentiation and impaired growth of AML cells. *Mol Cancer Ther*. 2017;16(2):273-284.
27. Maes T, Mascaró C, Tirapu I, et al. ORY-1001, a potent and selective covalent KDM1A inhibitor, for the treatment of acute leukemia. *Cancer Cell*. 2018; 33(3):495-511.e12.
28. Inoue A, Fujiwara T, Okitsu Y, et al. Elucidation of the role of LMO2 in human erythroid cells. *Exp Hematol*. 2013;41(12):1062-76.e1.
29. Zhong L, D'Urso A, Toiber D, et al. The histone deacetylase Sirt6 regulates glucose homeostasis via Hif1α. *Cell*. 2010;140(2):280-293.
30. Nagaoka K, Hino S, Sakamoto A, et al. Lysine-specific demethylase 2 suppresses lipid influx and metabolism in hepatic cells. *Mol Cell Biol*. 2015;35(7): 1068-1080.
31. Trapnell C, Pachter L, Salzberg SL. TopHat: discovering splice junctions with RNA-Seq. *Bioinformatics*. 2009;25(9):1105-1111.
32. Hino S, Sakamoto A, Nagaoka K, et al. FAD-dependent lysine-specific demethylase-1 regulates cellular energy expenditure. *Nat Commun*. 2012;3(1): 758.
33. Anan K, Hino S, Shimizu N, et al. LSD1 mediates metabolic reprogramming by glucocorticoids during myogenic differentiation. *Nucleic Acids Res*. 2018; 46(11):5441-5454.
34. Li H, Durbin R. Fast and accurate short read alignment with Burrows-Wheeler transform. *Bioinformatics*. 2009;25(14):1754-1760.
35. Heinz S, Benner C, Spann N, et al. Simple combinations of lineage-determining transcription factors prime cis-regulatory elements required for macrophage and B cell identities. *Mol Cell*. 2010;38(4):576-589.
36. Iacobucci I, Wen J, Meggendorfer M, et al. Genomic subtyping and therapeutic targeting of acute erythroleukemia. *Nat Genet*. 2019;51(4):694-704.
37. Ley TJ, Miller C, Ding L, et al; Cancer Genome Atlas Research Network. Genomic and epigenomic landscapes of adult de novo acute myeloid leukemia. *N Engl J Med*. 2013;368(22):2059-2074.


Downloaded from http://ashpublications.net/bloodadvances/article-pdf/5/9/2305/1806172/advancesadv2020003521.pdf by guest on 08 June 2024

38. Barretina J, Caponigro G, Stransky N, et al. The Cancer Cell Line Encyclopedia enables predictive modelling of anticancer drug sensitivity. *Nature*. 2012; 483(7391):603-607.

39. Bennett JM, Catovsky D, Daniel MT, et al. Proposals for the classification of the acute leukaemias. French-American-British (FAB) co-operative group. *Br J Haematol*. 1976;33(4):451-458.

40. Boddu P, Benton CB, Wang W, Borthakur G, Khoury JD, Pemmaraju N. Erythroleukemia-historical perspectives and recent advances in diagnosis and management. *Blood Rev*. 2018;32(2):96-105.

41. van Galen P, Hovestadt V, Wadsworth Ii MH, et al. Single-cell RNA-seq reveals AML hierarchies relevant to disease progression and immunity. *Cell*. 2019;176(6):1265-1281.e24.

42. van Wijk R, van Solinge WW, Nerlov C, et al. Disruption of a novel regulatory element in the erythroid-specific promoter of the human PKLR gene causes severe pyruvate kinase deficiency. *Blood*. 2003;101(4):1596-1602.

43. Oki S, Ohta T, Shioi G, et al. ChIP-Atlas: a data-mining suite powered by full integration of public ChIP-seq data. *EMBO Rep*. 2018;19(12):1-10.

44. Shimizu R, Engel JD, Yamamoto M. GATA1-related leukaemias. *Nat Rev Cancer*. 2008;8(4):279-287.

45. Avellino R, Havermans M, Erpelinck C, et al. An autonomous CEBPA enhancer specific for myeloid-lineage priming and neutrophilic differentiation. *Blood*. 2016;127(24):2991-3003.

46. Moriguchi T, Yamamoto M. A regulatory network governing Gata1 and Gata2 gene transcription orchestrates erythroid lineage differentiation. *Int J Hematol*. 2014;100(5):417-424.

47. Maiques-Diaz A, Spencer GJ, Lynch JT, et al. Enhancer activation by pharmacologic displacement of LSD1 from GFI1 induces differentiation in acute myeloid leukemia. *Cell Rep*. 2018;22(13):3641-3659.

48. Hu X, Li X, Valverde K, et al. LSD1-mediated epigenetic modification is required for TAL1 function and hematopoiesis. *Proc Natl Acad Sci USA*. 2009; 106(25):10141-10146.

49. Karia D, Gilbert RCG, Biasutto AJ, Porcher C, Mancini EJ. The histone H3K4 demethylase JARID1A directly interacts with haematopoietic transcription factor GATA1 in erythroid cells through its second PHD domain. *R Soc Open Sci*. 2020;7(1):191048.

50. Di Genua C, Valletta S, Buono M, et al. C/EBPα and GATA-2 mutations induce bilineage acute erythroid leukemia through transformation of a neomorphic neutrophil-erythroid progenitor. *Cancer Cell*. 2020;37(5):690-704.e8.

51. Kroemer G, Pouyssegur J. Tumor cell metabolism: cancer's Achilles' heel. *Cancer Cell*. 2008;13(6):472-482.

52. Kim Y, Nam HJ, Lee J, et al. Methylation-dependent regulation of HIF-1α stability restricts retinal and tumour angiogenesis. *Nat Commun*. 2016;7(1):1-14.

53. Shimizu R, Kuroha T, Ohneda O, et al. Leukemogenesis caused by incapacitated GATA-1 function. *Mol Cell Biol*. 2004;24(24):10814-10825.

54. Fagnan A, Bagger FO, Piqué-Borràs M-R, et al. Human erythroleukemia genetics and transcriptomes identify master transcription factors as functional disease drivers. *Blood*. 2020;136(6):698-714.

55. Leonards K, Almosailleakh M, Tauchmann S, et al. Nuclear interacting SET domain protein 1 inactivation impairs GATA1-regulated erythroid differentiation and causes erythroleukemia. *Nat Commun*. 2020;11(1):2807.

56. Ribeil J-A, Zermati Y, Vandekerckhove J, et al. Hsp70 regulates erythropoiesis by preventing caspase-3-mediated cleavage of GATA-1. *Nature*. 2007; 445(7123):102-105.

57. de Thonel A, Vandekerckhove J, Lanneau D, et al. HSP27 controls GATA-1 protein level during erythroid cell differentiation. *Blood*. 2010;116(1):85-96.

58. Zhang P, Iwasaki-Arai J, Iwasaki H, et al. Enhancement of hematopoietic stem cell repopulating capacity and self-renewal in the absence of the transcription factor C/EBP α. *Immunity*. 2004;21(6):853-863.

59. Loke J, Chin PS, Keane P, et al. C/EBPα overrides epigenetic reprogramming by oncogenic transcription factors in acute myeloid leukemia. *Blood Adv*. 2018;2(3):271-284.

60. Rapino F, Robles EF, Richter-Larrea JA, Kallin EM, Martinez-Climent JA, Graf T. C/EBPα induces highly efficient macrophage transdifferentiation of B lymphoma and leukemia cell lines and impairs their tumorigenicity [published correction appears in *Cell Rep*. 2017;19(6):1281]. *Cell Rep*. 2013;3(4): 1153-1163.

61. Nerlov C. C/EBPalpha mutations in acute myeloid leukaemias. *Nat Rev Cancer*. 2004;4(5):394-400.

62. Assi SA, Imperato MR, Coleman DJL, et al. Subtype-specific regulatory network rewiring in acute myeloid leukemia. *Nat Genet*. 2019;51(1):151-162.

63. Kreitz J, Schönfeld C, Seibert M, et al. Metabolic plasticity of acute myeloid leukemia. *Cells*. 2019;8(8):805.

64. Fang Y, Liao G, Yu B. LSD1/KDM1A inhibitors in clinical trials: advances and prospects. *J Hematol Oncol*. 2019;12(1):129.

Downloaded from http://ashpublications.net/bloodadvances/article-pdf/5/9/2305/1806172/advancesadv2020003521.pdf by guest on 08 June 2024